

Doppler optical coherence tomography monitoring of microvascular tissue response during photodynamic therapy in an animal model of Barrett's esophagus

Beau A. Standish, BEng, Victor X. D. Yang, MD, PhD, Nigel R. Munce, MSc,
Louis-Michel Wong Kee Song, MD, Geoffrey Gardiner, MD, Annie Lin, MD, Youxin I. Mao, PhD,
Alex Vitkin, PhD, Norman E. Marcon, MD, Brian C. Wilson, PhD

Toronto, Ontario, Canada

Background: Doppler optical coherence tomography (DOCT) is an imaging modality that allows assessment of the microvascular response during photodynamic therapy (PDT) and may be a powerful tool for treatment monitoring/optimization in conditions such as Barrett's esophagus (BE).

Objective: To assess the technical feasibility of catheter-based intraluminal DOCT for monitoring the microvascular response during endoluminal PDT in an animal model of BE.

Design: Thirteen female Sprague-Dawley rats underwent esophagojejunostomy to induce enteroesophageal reflux for 35 to 42 weeks and the formation of Barrett's mucosa. Of these, 9 received PDT by using the photosensitizer Photofrin (12.5 mg/kg intravenous), followed by 635-nm intraluminal light irradiation 24 hours after drug administration. The remaining 4 surgical rats underwent light irradiation without Photofrin (controls). Another group of 5 normal rats, without esophagojejunostomy, also received PDT. DOCT imaging of the esophagus by using a catheter-based probe (1.3-mm diameter) was performed before, during, and after light irradiation in all rats.

Results: Distinct microstructural differences between normal squamous esophagus, BE, and the transition zone between the 2 tissues were observed on DOCT images. Similar submucosal microcirculatory effects (47%-73% vascular shutdown) were observed during PDT of normal esophagus and surgically induced BE. Controls displayed no significant microvascular changes.

Conclusions: No apparent difference was observed in the PDT-induced vascular response between normal rat esophagus and the BE rat model. Real-time monitoring of PDT-induced vascular changes by DOCT may be beneficial in optimizing PDT dosimetry in patients undergoing this therapy for BE and other conditions. (Gastrointest Endosc 2007;66:326-33.)

Doppler optical coherence tomography (DOCT)^{1,2} is an imaging modality that combines the high spatial resolution of optical coherence tomography (OCT)³ and Doppler measurement of blood flow, with a velocity resolution down to approximately 20 $\mu\text{m/s}$.⁴ This technology has enabled the detection of blood flow noninvasively in human retina,⁵ skin,⁶ and the GI tract,⁷ as well as providing cross-sectional images of tissue at near-histologic resolution. In particular, fiber-optic implementation allows endoscopic imaging, as previously reported by us⁷ in patients under-

going surveillance for Barrett's esophagus (BE), a condition in which the normal squamous mucosa is replaced by columnar, intestine-like mucosa and in which there is a marked increase in the risk of dysplasia, a precursor of esophageal adenocarcinoma.⁸

Photodynamic therapy (PDT) involves light activation of an administered photosensitizer that reacts with molecular oxygen, generating reactive oxygen species, causing necrosis and/or apoptosis of cells,⁹ activation of the host immune system,¹⁰ and vascular damage.^{11,12} These effects depend on the photosensitizer, the target tissue, and the specific treatment parameters. In the case of PDT for destruction of solid malignant tumors, vascular shutdown can induce tissue ischemia, leading to tumor-cell death.

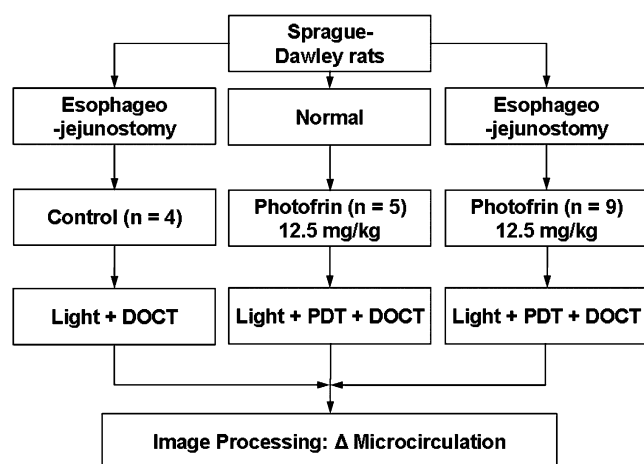


Figure 1. Group allocation of normal and surgically altered rats.

If light activation is carried out shortly after photosensitizer administration (while the drug is still confined to the vasculature), then vascular shutdown is the primary mode of action. This is the case, for example, in PDT for age-related macular degeneration (choroidal neovascularity)¹³ when using Visudyne (Visudyne, East Hanover, NJ) and for prostate cancer when using TOOKAD (Steba Biotech, Paris, France). PDT is approved for the treatment of certain GI conditions, including palliation of esophageal cancer and treatment of BE with high-grade dysplasia (HGD) by using the first-generation photosensitizer Photofrin (Axcan Pharma, Montreal, Quebec, Canada).^{14,15} Microcirculatory changes, including vascular shutdown, were reported as a mechanism responsible for the PDT treatment effect.¹³ Previously, we reported on DOCT monitoring of the PDT-induced vascular effects during laparotomy in normal rats.¹⁶ We also recently demonstrated a novel DOCT system capable of imaging the microcirculation in both the animal (rat)¹⁷ and human GI tracts,⁷ and its feasibility for endoscopic use.⁷

The primary aim of the present study was to demonstrate the technical feasibility of DOCT to monitor the vascular changes that occurred during endoluminal PDT in a BE rat model. With the study design including a BE arm and a normal arm, a secondary aim was to assess whether BE and normal esophageal vasculature responded differently to PDT.

MATERIALS AND METHODS

Animals and PDT

All animal procedures were carried out, with institutional approval, at the University Health Network, Toronto, Canada. Female Sprague-Dawley rats (180-250 g) were purchased (Harlan, Indianapolis, Ind) and housed 2 per cage under standard laboratory conditions. To the best of our knowledge, it has not been previously shown that the choice of sex for inducing BE via esophageo-jejunostomy is of great importance. We, therefore, chose the more docile female sex, because the animal handling time for this study was extensive (BE formation took >35 weeks). The rats were maintained on a high protein (Ensure; Abbott, Montreal, Canada) and mushed Kibble (KMR; PetAg, Hampshire, Ill) diet. The rat's food was withheld for 24 hours before surgical intervention and before DOCT imaging. Thirteen rats underwent esophageo-jejunostomy by using the Levrat technique, as previously described in detail,^{18,19} to induce enteroesophageal reflux for 35 to 42 weeks and the subsequent formation of Barrett's epithelium. Briefly, the rats were anesthetized with xylazine hydrochloride (12 mg/kg intramuscular [IM]) and ketamine (75 mg/kg IM). A midline laparotomy was performed, the gastroesophageal junction was ligated, and the distal esophagus was transected 2 mm above the ligature. To stabilize the esophagus, a soft silicone tube was placed into the esophagus down as far as the gastroesophageal junction before transection. A jejunostomy was created just distal to the ligament of Treitz, and an end-to-side esophageo-jejunostomy was constructed with accurate mucosa-to-mucosa approximation. Analgesia (buprenorphine) was administered after surgery, and the rats were fed by the first postoperative day.

Normal and surgically altered (BE) rats were randomized into 3 groups, as shown in Figure 1. Nine surgically altered rats and 5 normal rats were administered the photosensitizer Photofrin at 12.5 mg/kg intravenous, 24 hours before light irradiation. For treatment, a 0.8-mm-diameter, 2.7-cm-long, cylindrical, diffusing fiber was placed into the esophagus to deliver a 635-nm minimum total irradiance of 37 J cm⁻² at 45 mW cm⁻². Four rats in the BE group received the same light irradiation without Photofrin (controls). The rats were euthanized with a 0.5 mL intracardiac injection of euthenol 24 hours after treatment, and the esophagus and the stomach were resected en bloc for histology.

Capsule Summary

What is already known on this topic

- One of the mechanisms of Photofrin-based photodynamic therapy, which can be used for treatment of Barrett's esophagus (BE), is the vasoconstrictive effect of such therapy on tissue microvasculature and associated tissue ischemia.

What this study adds to our knowledge

- When using Doppler optical coherence tomography imaging in a rat model, there were distinct microstructural differences among normal squamous esophagus, BE, and their transition zone.
- Similar submucosal microcirculatory effects were observed in normal esophagus and surgically induced BE after photodynamic therapy.

DOCT imaging

The technical specifications of the DOCT system were reported previously.^{4,16} Briefly, a customized catheter-based fiber-optic probe (1.3-mm outer diameter) was constructed, the distal end of which was terminated by a side-viewing ball lens (300- μ m diameter). The optical fiber was translated along the catheter by a scanning motor, which provided cross-sectional images of the esophagus that measured approximately 2 mm (lateral) by 1.5 mm (depth). The measured beam-spot size of the ball lens was 22.5 μ m (y -axis) and 29.3 μ m (x -axis).²⁰ The depth resolution of the DOCT system was 10 μ m in tissue, and the minimum detectable blood velocity was approximately 100 μ m/s, as calculated via a color-Doppler imaging algorithm.⁴ We assumed a Doppler angle of $\pm 60^\circ$ when a particular image did not allow for the determination of the Doppler angle; this was labeled "velocity*." Velocity variance images were also acquired, which can potentially quantify flow as fast as 10 cm/s while maintaining sensitivity to microcirculation.⁴

DOCT imaging was performed before, during, and after light irradiation in all rats. The DOCT probe was positioned alongside the cylindrical diffusing PDT fiber in the esophagus, under fluoroscopic guidance. Structural, color-Doppler, and velocity variance images were acquired continuously at 1 fps and were separated into 3 stages: before ($t = 0$ -2 minutes), during ($t = 2$ -27 minutes), and after ($t = 27$ -30 minutes) light irradiation. Motion artifacts induced by the heart beat, breathing, and peristalsis of the esophagus can dominate the true Doppler signal, because these movements can be much faster than that of the red blood cells. Therefore, an image segmentation algorithm was used to remove these motion artifacts.²¹ Briefly, the first step involved a velocity histogram segmentation of the color-Doppler image to remove bulk-tissue motion, followed by structural intensity thresholding. The cross-sectional areas of the detected vasculature were measured by pixel counts of the color-Doppler images. These values were averaged over 1-minute intervals during the DOCT imaging session and were defined as the vascular index. The vascular index was normalized, and the changes in detected blood flow were quantified by analyzing the DOCT data for the 3 stages.

Histologic correlation

Care was taken in measuring the length of the DOCT probe that entered the esophagus during intubation under fluoroscopic guidance. Once the probe was positioned alongside the diffusing fiber, it was marked at a point where the probe entered the mouth of the rat. After its removal, the distance from the probe's ball lens to the proximal marked area was measured. This measurement was then used during esophageal resection, 24 hours after PDT, for locating the region imaged by the DOCT system. The resected samples were processed by standard

histologic methods and were stained with hematoxylin and eosin.

Image interpretation

One OCT scientist and 1 GI pathologist (G.G.) reviewed the OCT and histologic images, respectively. The GI pathologist was blinded to the rat group assignment (BE, normal, or control) and to the measurement results. All DOCT images were analyzed in the rat groups (BE, normal, or control) as they were originally assigned. The endoscopist was not blinded to the rat group assignment but was blinded to the vascular index analysis, which was performed automatically, without input from the endoscopist. In this feasibility study, we did not aim to make subgroup diagnosis in the rats in the BE group, such as low-grade dysplasia, HGD, or invasive cancer. Therefore, interobserver reproducibility analysis was not part of the study.

RESULTS

DOCT images and histologic correlation

Microstructural and microvascular features of the normal rat esophagus were readily identified by DOCT and were easily correlated with the histologic features, as shown in Figure 2. Under DOCT imaging, the normal esophagus displayed a distinct multilayered structure, with identification of epithelium, lamina propria, muscularis mucosa, submucosa, muscularis propria interna, muscularis propria externa, and serosa (Fig. 2B). Blood vessels located between the muscularis propria interna and the muscularis propria externa were readily apparent, and counter-propagating blood flow was also imaged in this region, as shown by the color-coded regions in the Doppler imaging mode (Fig. 2C).

Substantial microstructural and microvascular differences were observed with DOCT imaging when normal esophagus, BE, and their respective transition zones were compared in the surgically altered rats. An example of a color-Doppler blood-flow image in normal rat esophagus is shown in Figure 3A, whereas Figure 3B is an example of a velocity-variance blood-flow image in a squamocolumnar transition zone. Multiple scattering of photons through large vessels may contribute to the large streak in Figure 3B, which typically occurs below a large vessel, as was previously reported.²² Glandular structures and loss of distinct tissue layers were observed in BE compared with normal esophagus (Fig. 3C and D). These features are typical OCT markers for BE, as previously described.^{7,23,24}

DOCT vascular index during PDT

Typical velocity and color-Doppler images obtained before, during, and after the course of a PDT treatment are shown in Figure 4. The vascular indices for all 3 groups studied are summarized in Figure 5. Minimal changes

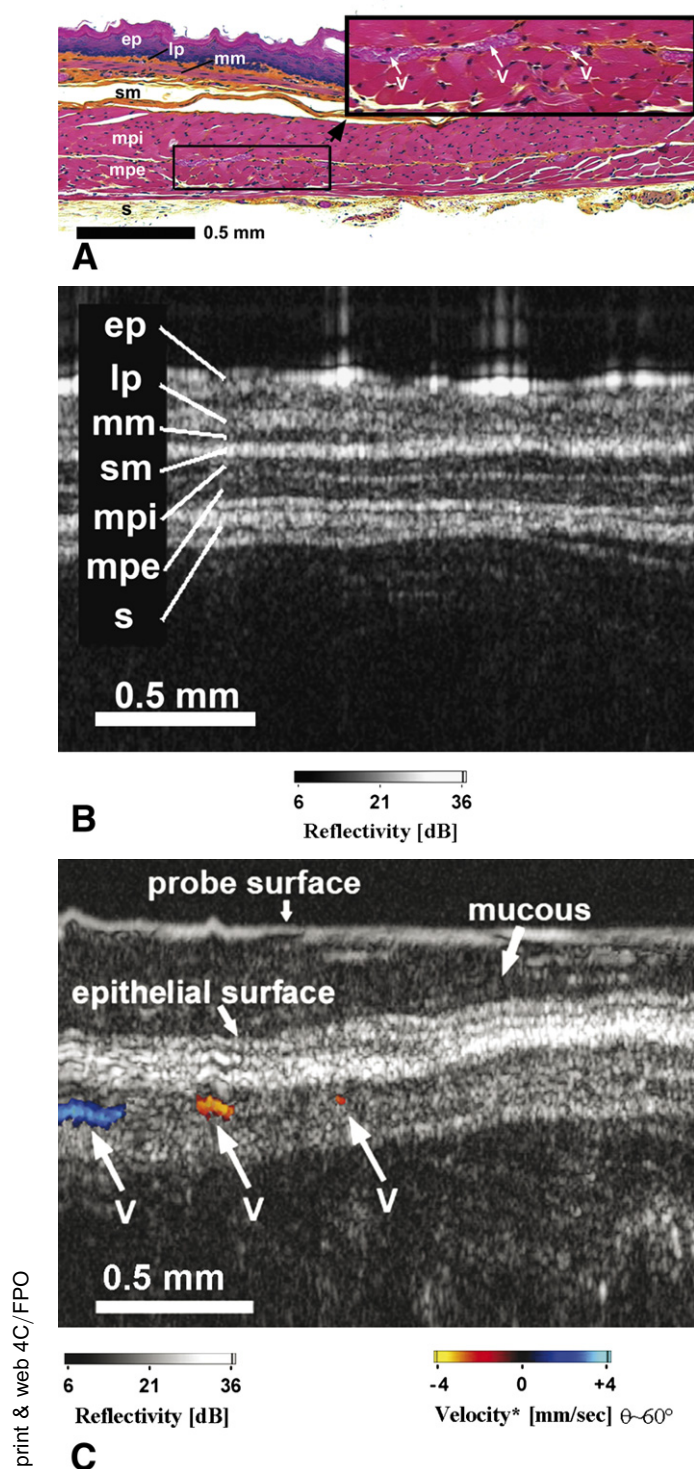


Figure 2. Histology and corresponding in vivo DOCT images of a normal rat esophagus. **A**, Histologic layers, *inset* is a magnified view of blood vessels (V) within the muscularis propria (hematoxylin phloxine saffron, orig. mag. $\times 20$). **B**, Microstructural DOCT image of the corresponding esophageal layers. **C**, Composite image with the Doppler shift of blood vessels overlaid on the microstructural OCT image. The visible esophageal layers are the following: *ep*, epithelium; *lp*, lamina propria; *mm*, muscularis mucosa; *sm*, submucosa; *mpi*, muscularis propria interna; *mpe*, muscularis propria externa, and *s*, serosa. *Velocity** assumes a Doppler angle of $\pm 60^\circ$.

were noted in the vascular index of the control group (BE + light only) during and after light exposure (Fig. 5C). A noticeable reduction in the vascular index, however, was observed in the BE group that received PDT (BE + Photofrin + light) (Fig. 5A). During PDT, an average reduction of $57\% \pm 10\%$ (\pm standard error) in the vascular index was measured, with partial recovery in the post-PDT period. A similar phenomenon was observed in the group of normal rats that received PDT (Fig. 5B), with an average decrease of $63\% \pm 10\%$ (\pm standard error) in the vascular index. There was little difference when comparing the PDT-induced vascular response between the 2 groups.

Statistics

Although the sample sizes were small in this study, null hypothesis testing (independent *t* test) was applied to the normalized DOCT vascular index quantity at the 15- and 30-minute time points (Fig. 5) between group allocations. The control group (BE + light) was found to be statistically different ($P < .05$) from all other groups at the 15- and 30-minute time points. Although the PDT vascular response of the normal and BE groups were very similar, they were also found to be statistically different ($P < .05$) at the 15-minute ($P = .06$) and 30-minute ($P = .83$) time points.

Safety

There were no animal complications or technical difficulties as a result of PDT treatment or DOCT imaging during this study.

DISCUSSION

PDT when using Photofrin is U.S. Food and Drug Administration approved for the treatment of patients with Barrett's esophagus with HGD. In a previous study, a significant difference in the eradication of HGD was found between a Photofrin-PDT plus omeprazole (proton pump inhibitor) group and an omeprazole-only control group, 77% vs 39%, respectively ($P < .0001$). However, residual Barrett's epithelium remained in 48% of patients treated with PDT, and, in 13% of the cases, cancer eventually developed.²⁵ Moreover, the persistence of genetic abnormalities in residual BE and the presence of islands of BE buried underneath the neosquamous epithelium represent a risk of progression to esophageal adenocarcinoma.²⁶ Given these concerns, the goal of PDT should be to eradicate the entire Barrett's epithelium,²⁷ and this may be facilitated by real-time monitoring of PDT-induced tissue responses to allow adjustment and optimization of the PDT dose.

The efficacy of PDT is partly dependent on its vasoconstrictive effect on tissue microvasculature and associated tissue ischemia. Transient reduction in blood flow or permanent vessel occlusion occurs as a result of PDT-induced vascular spasm, vascular stasis, platelet aggregation, and

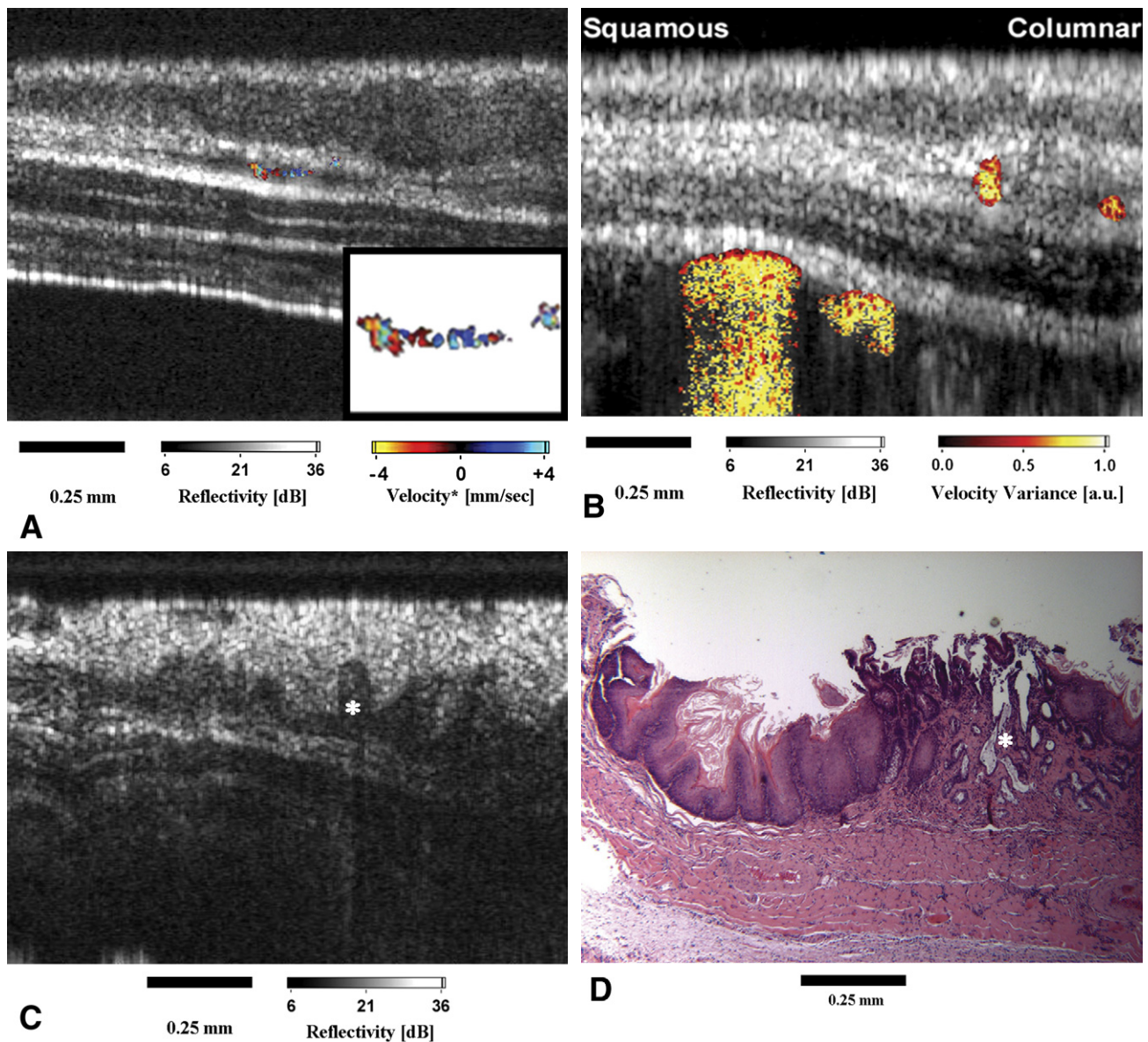


Figure 3. DOCT images. **A**, Normal rat with subepithelial detection of blood vessel represented by the color-Doppler image overlaid onto structural image; inset is a $\times 2$ magnification of the detected vessels. **B**, Squamocolumnar transition zone with the velocity variance image overlaid onto structural image; multiple scattering of photons through large vessels contribute to the large streak, which typically occur deeper to a large vessel. **C**, Structural BE OCT image. **D**, Histologic correlate of transition zone with Barrett's glandular structures identified (asterisks in **C** and **D**) (H&E, orig. mag. $\times 10$). Differences in blood flow were detected between the tissues (**A** and **B**).

thrombus formation.^{28,29} The observation and quantification of these microvascular alterations by a noninvasive imaging device in real time could be an important surrogate marker for determining and optimizing the overall therapeutic efficacy of PDT in BE and other sites. DOCT appears well suited for this purpose, because it offers high spatial resolution (approximately $10\ \mu\text{m}$) and excellent blood-flow velocity sensitivity (approximately $100\ \mu\text{m/s}$ in vivo), providing unique noninvasive microstructural and functional imaging when compared with existing endoscopic imaging methods, such as EUS.

The data presented here demonstrated the feasibility of using DOCT to monitor the tissue microvascular response during PDT in BE and normal esophagus. Vascular compromise was observed and quantified by DOCT during PDT of both normal and BE tissues. There were statistical differences in the Photofrin-PDT vascular response between the 2 groups at the 15- and 30-minute point of the treatment session, with the PDT treatment conditions used here. However, this feasibility study was not statistically powered to detect small differences. We also noted that, with the 24-hour Photofrin-light interval used here,

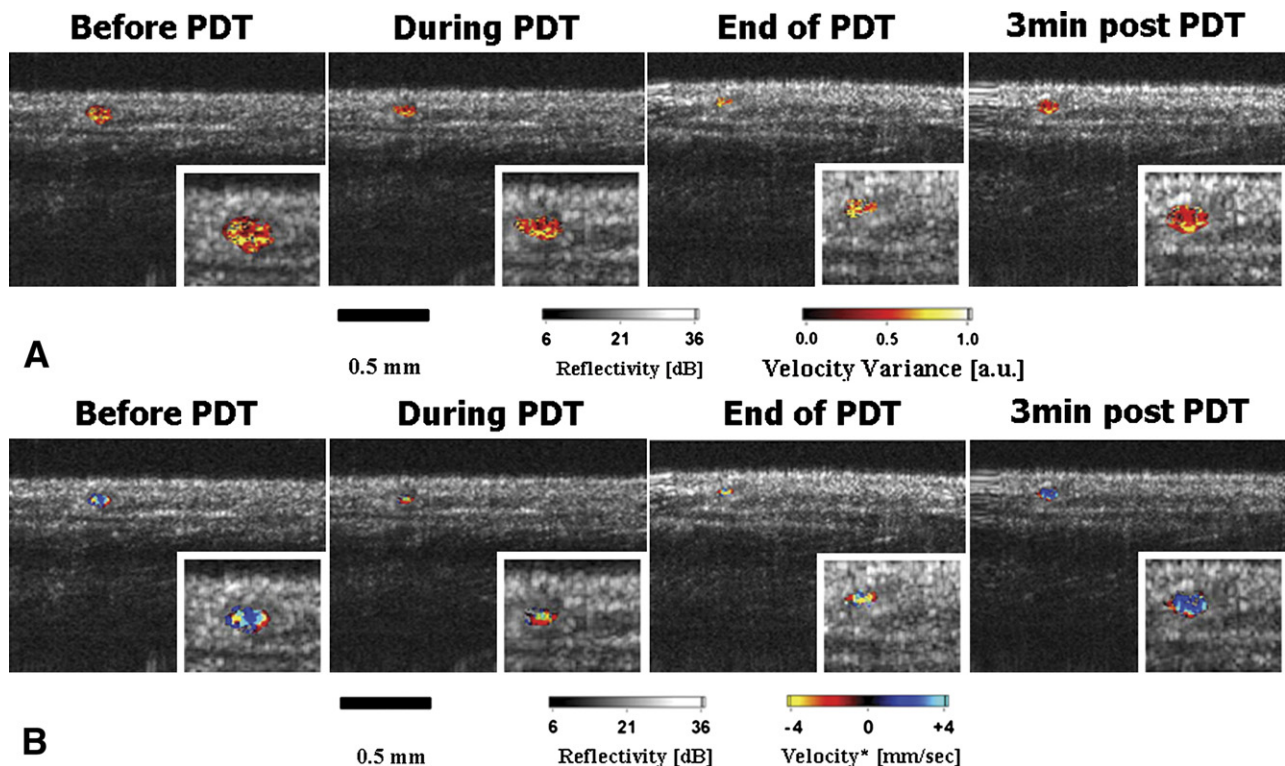


Figure 4. DOCT monitoring of the esophagus before (0-2 minutes), during (2-27 minutes), and after (27-30 minutes) PDT light exposure, for a total imaging time of 30 minutes. *Inset boxes* represent $\times 1.5$ magnification of the detected blood vessel. **A**, Blood flow is color coded by the detected velocity variance images; a noticeable reduction in the vascular index was seen during treatment, with recovery in the posttreatment period. **B**, Color-Doppler images of corresponding vessel.

there was likely both vascular and a direct cell-kill component in the tissue response. Whether these observations hold in our planned larger study with a predominantly vascular photosensitizer (ie, TOOKAD), remains to be seen.

As previously shown,⁷ the DOCT system is suitable for human endoscopic applications, and work is underway regarding the transfer of this technology for use in patients with Barrett's esophagus who are undergoing PDT. Initial clinical studies will correlate DOCT parameters (eg, different vascular indices) to the degree of eradication of Barrett's epithelia after Photofrin-PDT, and the determination of DOCT thresholds at which complete Barrett's esophagus eradication is observed. A technical issue with DOCT is the system's inability to visualize Doppler signals from microvessels because of bulk-tissue motion, Doppler-angle dependencies, and variations in blood-flow dynamics (eg, intermittent flow). Although we currently use a bulk-tissue rejection algorithm, this process may not be optimized, resulting in omitted vessels. To circumvent this, we are currently investigating clutter rejection algorithms to be used in angle-independent power Doppler (PD) signal processing for OCT. Furthermore, with the addition of temporal averaging, PD-OCT may also limit the effects of variations in blood-flow dynamics, improving our ability to visualize and quantify microvessels. Future prospective studies will include real-time DOCT monitoring

and PDT parameter adjustment (eg, total irradiance and/or irradiation time) to achieve the desired DOCT thresholds and their influence on the completeness of Barrett's esophagus eradication. As a first step to investigate the vascular effects of varying PDT parameters, we recently published a light dose-escalation study in a prostate cancer model,³⁰ in which we observed irradiance (rate) dependencies of DOCT-detected vascular shutdown resulting from of PDT. These results demonstrated the feasibility of using DOCT to detect changes in vasculature as a function of varying PDT parameters. A similar escalation study by using rats with BE may provide the necessary data to outline a protocol for optimizing PDT in BE. Three-dimensional volumetric perfusion measurements of the PDT-induced vascular response may improve DOCT measurement accuracy, and this is also being explored. Finally, DOCT is currently being used to study and compare the effects of other photosensitizers on tissue microvascular responses.

In this study, we demonstrated the feasibility of DOCT to detect, monitor, and quantify microvascular changes during PDT. The DOCT imaging system provided a unique opportunity to assess the effects of PDT on tissue microvasculature, a likely key determinant in its overall therapeutic efficacy. Although we and other investigators have reported on DOCT monitoring of microcirculatory changes in animals and human beings, to the best of

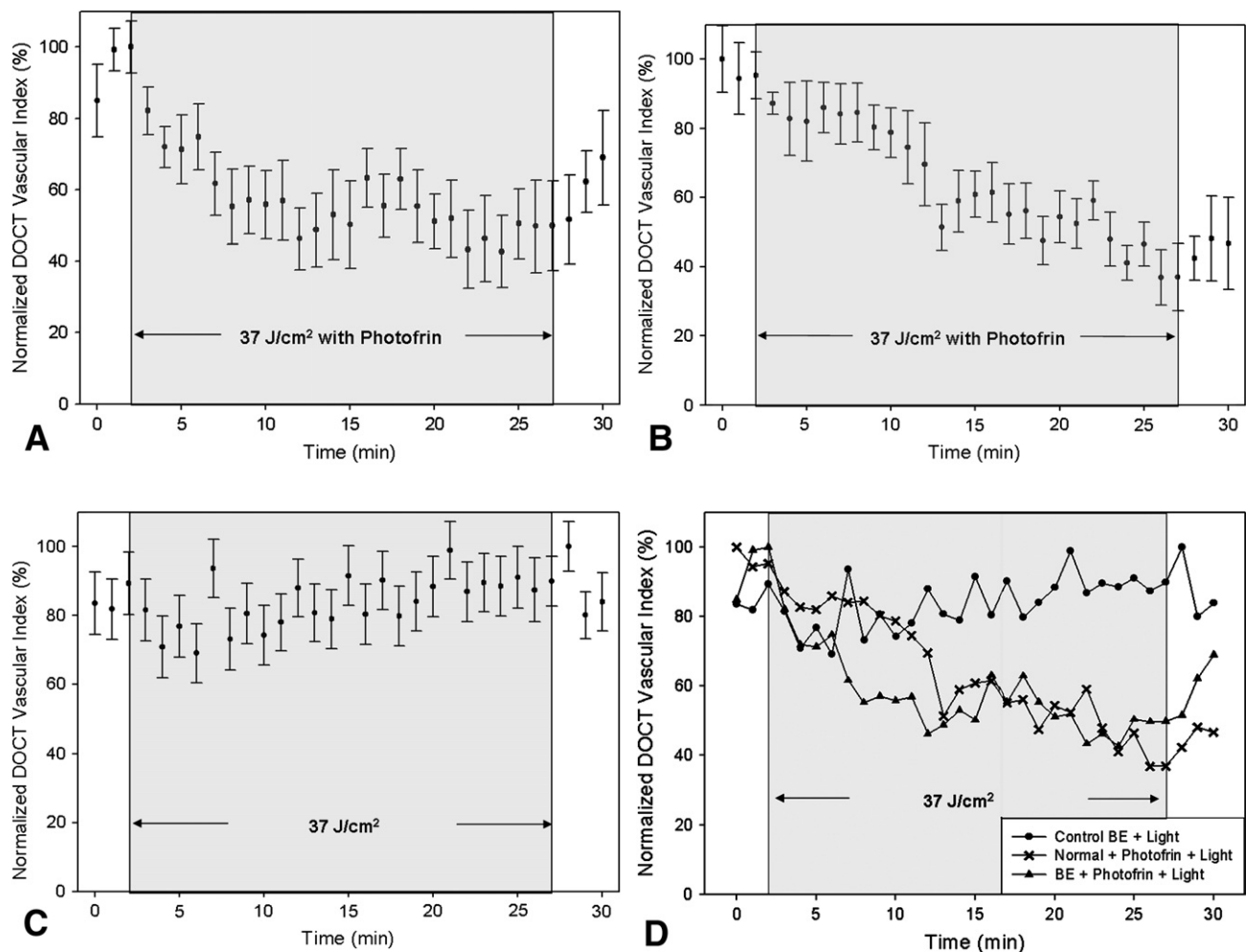


Figure 5. **A**, Normalized DOCT average vascular index (\pm standard error, interanimal) before (0-2 minutes), during (2-27 minutes), and after (27-30 minutes) light irradiation in the rat model of BE. The gray-shaded box represents the 25-minute light irradiation interval. **B**, Corresponding measurements in the normal rat esophagus. **C**, Corresponding measurements in the control rats (light/no Photofrin). **D**, Summary graph for the 3 groups.

our knowledge, this is the first report of a catheter-based intraluminal DOCT study for vascular monitoring. This feasibility study lays the ground work for using DOCT as a real-time, noninvasive monitoring device for PDT in patients with Barrett's esophagus.

ACKNOWLEDGMENTS

We thank Dr Stuart Bisland from the Ontario Cancer Institute and Drs Navtej S. Buttar and Kenneth K. Wang from the Mayo Clinic, Rochester, Minnesota, for their advice and assistance.

DISCLOSURE

None of the authors have any disclosures to make. Supported by the Canadian Cancer Society through

a grant from the National Cancer Institute of Canada. Doppler optical coherence tomography development was supported by the Canadian Institutes for Health Research, the Canadian Foundation for Innovation, Photonics Research Ontario, the Gordon Lang Foundation and the Natural Sciences and Engineering Research Council of Canada.

REFERENCES

1. Yazdanfar S, Kulkarni MD, Izatt JA. High resolution imaging of in vivo cardiac dynamics using color Doppler optical coherence tomography. *Opt Express* 1997;1:424-31.
2. Chen Z, Milner TE, Dave D, et al. Optical Doppler tomographic imaging of fluid flow velocity in highly scattering media. *Opt Lett* 1997;1:64-6.
3. Huang D, Swanson EA, Lin CP, et al. Optical coherence tomography. *Science* 1991;254:1178-81.

4. Yang VXD, Gordon ML, Qi B, et al. High speed, wide velocity dynamic range Doppler optical coherence tomography (Part 1): system design, signal processing, and performance. *Opt Express* 2003;4:794-809.
5. Yazdanfar S, Rollins AM, Izatt JA. Imaging and velocimetry of the human retinal circulation with color Doppler optical coherence tomography. *Opt Lett* 2000;25:1448-50.
6. Zhao Y, Chen Z, Saxer C, et al. Phase-resolved optical coherence tomography and optical Doppler tomography for imaging blood flow in human skin with fast scanning speed and velocity sensitivity. *Opt Lett* 2000;25:114-6.
7. Yang VXD, Tang S, Gordon ML, et al. Endoscopic Doppler optical coherence tomography in the human GI tract: initial experience. *Gastrointest Endosc* 2005;61:879-90.
8. Haggitt RC. Barrett's esophagus, dysplasia, and adenocarcinoma. *Hum Pathol* 1994;25:982-93.
9. Oleinick NL, Morris RL, Belichenko I. The role of apoptosis in response to photodynamic therapy: what where, why, and how. *Photochem Photobiol Sci* 2002;1:1-21.
10. Van Duijnhoven FH, Aalvers RI, Rovers JP, et al. The immunological consequences of photodynamic treatment of cancer, a literature review. *Immunobiology* 2003;207:105-13.
11. Chen B, Pogue BW, Goodwin IA, et al. Blood flow dynamics after photodynamic therapy with verteporfin in the RIF-1 tumor. *Radiat Res* 2003;160:452-9.
12. Finger V, Wieman T, Wiehle S, et al. The role of microvascular damage in photodynamic therapy: the effect of treatment on vessel constriction, permeability, and leukocyte adhesion. *Can Res* 1992;52:4914-21.
13. van den Bergh H, Ballini JP, Sickenberg M. On the selectivity of photodynamic therapy of choroidal neovascularization associated with age-related macular degeneration. *J Fr Ophtalmol* 2004;27:75-8.
14. Overholt BF, Panjehpour M, DeNovo RC, et al. Photodynamic therapy for esophageal cancer using a 180 degrees windowed esophageal balloon. *Lasers Surg Med* 1994;14:27-33.
15. Huang Z. A review of progress in clinical photodynamic therapy. *Technol Cancer Res Treat* 2005;4:283-93.
16. Gordon ML, Yang VXD, Seng Yue E, et al. Doppler optical coherence tomography for monitoring the vascular effects of photodynamic therapy. *Proc SPIE* 2004;5316:147-54.
17. Yang VXD, Gordon ML, Tang S, et al. High speed, wide velocity dynamic range Doppler optical coherence tomography (Part III): in vivo endoscopic imaging of blood flow in the rat and human gastrointestinal tracts. *Opt Express* 2003;11:2416-25.
18. Pera M, Trastek VF, Carpenter HA, et al. Influence of pancreatic and biliary reflux on the development of esophageal carcinoma. *Ann Thorac Surg* 1993;55:1386-93.
19. Buttar NS, Wang KK, Leontovich O, et al. Chemoprevention of esophageal adenocarcinoma by COX-2 inhibitors in an animal model of Barrett's esophagus. *Gastroenterology* 2002;122:1101-12.
20. Yang VXD, Mao YX, Munce N, et al. Interstitial Doppler optical coherence tomography. *Opt Lett* 2005;30:1791-3.
21. Yang VX, Gordon ML, Mok A, et al. Improved phased-resolved optical Doppler tomography using the Kasai velocity estimator and histogram segmentation. *Opto Commun* 2002;208:202-14.
22. Zhao Y, Chen Z, Saxer C, et al. Phase-resolved optical coherence tomography and optical Doppler tomography for imaging blood flow in human skin with fast scanning speed and high velocity sensitivity. *Opt Lett* 2000;25:114-6.
23. Poneros JM, Brand S, Bouma BE, et al. Diagnosis of specialized intestinal metaplasia by optical coherence tomography. *Gastroenterol* 2001;120:219-24.
24. Evans JA, Poneros JM, Bouma BE, et al. Optical coherence tomography to identify intramucosal carcinoma and high-grade dysplasia in Barrett's esophagus. *Clin Gastroenterol Hepatol* 2006;4:38-43.
25. Overholt BF, Lightdale CJ, Wang KK, et al. International Photodynamic Group for High-Grade Dysplasia in Barrett's Esophagus. Photodynamic therapy with porfimer sodium for ablation of high-grade dysplasia in Barrett's esophagus: international, partially blinded, randomized phase III trial. *Gastrointest Endosc* 2005;62:488-98.
26. Hage M, Siersema PD, Vissers KJ, et al. Genomic analysis of Barrett's esophagus after ablative therapy: persistence of genetic alterations at tumor suppressor loci. *Int J Cancer* 2006;118:155-60.
27. Siersema PD. Photodynamic therapy for Barrett's esophagus: not yet ready for the premier league of endoscopic interventions. *Gastrointest Endosc* 2005;62:503-7.
28. Finger V, Wieman T, Wiehle S, et al. The role of microvascular damage in photodynamic therapy: the effect of treatment on vessel constriction, permeability, and leukocyte adhesion. *Cancer Res* 1992;52:4914-21.
29. Chen B, Pogue BW, Goodwin IA, et al. Blood flow dynamics after photodynamic therapy with verteporfin in the RIF-1 tumor. *Radiat Res* 2003;160:452-9.
30. Standish BA, Jin X, Smolen J, et al. Interstitial Doppler optical coherence tomography monitors microvascular changes during photodynamic therapy in a Dunning prostate model under varying treatment conditions. *J Biomed Opt* 2007;12:034022.

Received October 23, 2006. Accepted February 18, 2007.

Current affiliations: Department of Medical Biophysics (B.A.S., N.R.M., A.V., B.C.W.), Department of Radiation Oncology (A.V.), University of Toronto, Ontario Cancer Institute/University Health Network (V.X.D.Y., Y.I.M., A.V., B.C.W.), Department of Pathology (G.G.), Division of Gastroenterology (N.E.M.), St. Michael's Hospital, Toronto, Ontario, Canada, Division of Gastroenterology and Hepatology (L-M.W.), Mayo Clinic, Rochester, Minnesota, USA.

Presented at Digestive Disease Week, May 14-19, 2005, Chicago, Illinois (*Gastroenterology* 2005;128[Suppl 2]:A27).

Reprint requests: Beau A. Standish, Division of Biophysics and Bioimaging, Ontario Cancer Institute, 610 University Ave, Toronto, ON, Canada M5G 2M9.